P133

Investigating the Role of Wave-like Reflectivity Segments during the 17 November 2013 EF-4 Washington, Illinois Tornado

Edward J. Shimon III

National Weather Service Central Illinois, Lincoln Illinois

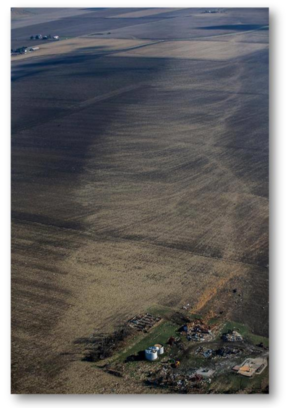

1. Introduction

Interactions of weak, wave-like reflectivity segments (WRS) with convection appear to be a common feature in severe weather environments. This is important since their interactions with convection are often followed by increases in severe weather, such as tornadoes. For example, Barker (2006) found a link between "reflectivity tags" (which were assumed to be waves) that moved quickly through linear convection and were associated with tornadogenesis. Coleman and Knupp (2006) documented mergers between linear features in radar reflectivity and convection that were temporally correlated with an increase in mesocyclone rotation or tornadogenesis. Murphy et. al. (2014) studied the frequency of tornadoes correlated with WRSs in the 2005-2012 years across the Tennessee Valley. They found that WRSs occurred on roughly two-thirds of the tornado days. Of all 236 tornadoes in their study, 23% were spatially and temporally correlated with a WRS-convection interaction.

This study will investigate the evidence of WRS interactions with the supercell that produced an EF-4 tornado on 17 November 2013 that devastated Washington IL.

2. Wave Background

Coleman and Knupp (2008) utilized a simple model and observations to show how the interaction of ducted gravity waves with a mesocyclone could increase the vertical vorticity (ζ) of the low-level mesocyclone. They showed that the ζ increase occurred through low-level vorticity stretching due to convergence ahead of wave ridges and/or the tilting of horizontal vorticity into the vertical associated with perturbation wind shear in the wave ridges (left and right figures below).

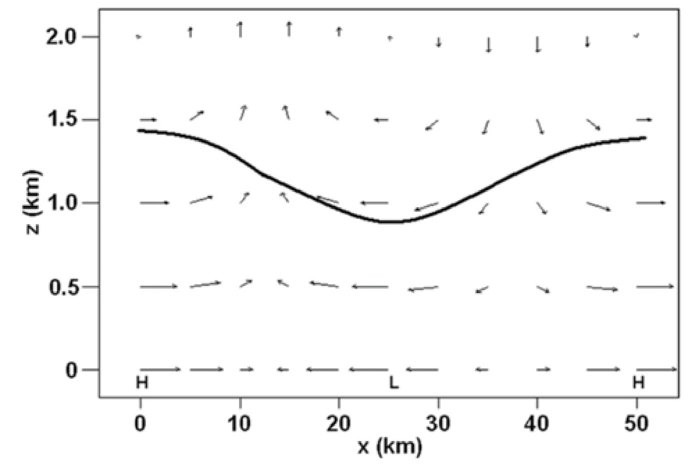

Left Figure - Airflow vectors and an isentrope (heavy solid curve) in the x-z plane for a ducted gravity wave with a wave duct just above 2 km. Divergence is largest near the surface, with convergence located ahead of a wave ridge and divergence ahead of a wave trough. Positive perturbation wind shear is centered in the wave trough and negative shear centered in the ridge. Coleman and Knupp (2008)

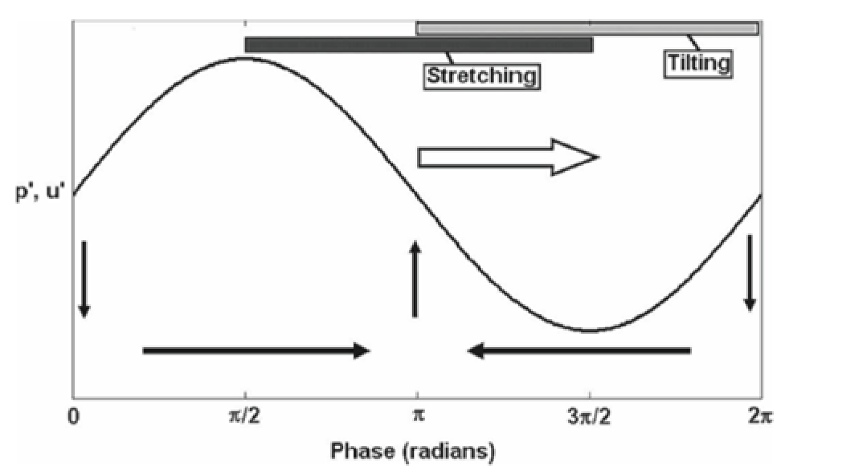

Right Figure - Regions of expected positive wave-induced stretching and tilting through interaction with a mesocyclone, relative to the gravity wave phase. Coleman and Knupp (2008)

Murphy and Knupp (2013) conducted the first in-depth kinematic analysis of WRS interaction with mesocyclones. Their major findings included the presence of enhanced horizontal vorticity within the WRSs, which trajectory analyses indicated entered the convective core of the QLCS during interaction, subsequently followed by an increase in the vertical vorticity of the convective core, and led to tornadogenesis.

They defined a WRS as:

- An area of weak-to-moderate radar reflectivity (between 10 and 40-45 dBZ)
- Major axis dimension much greater than minor axis (i.e., linear radar appearance; typically, but not always, oriented in east-west direction)
- Moving faster than component of the background wind in their direction of motion (i.e., exhibits propagation in addition to advection)
- Exhibits significant pressure perturbations (≥ 0.5-1.0hPa) at the surface.

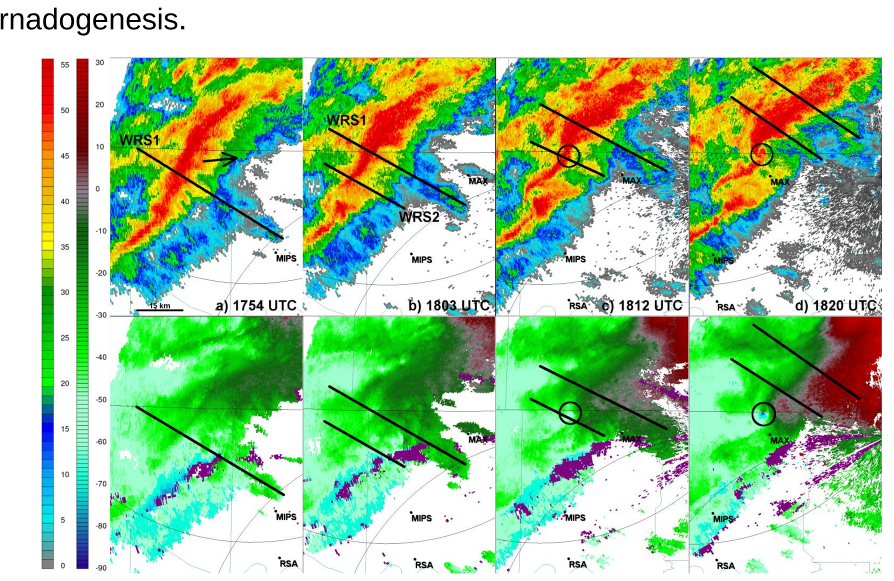

Z (top) and VR (bottom) at 0.5° from KHTX showing the evolution of the QLCS due to interaction with WRSs. Black lines and circles indicate the approximate center point of WRS 1 and 2 propagating through the convection and areas of rotation in VR, respectively. An EF-1 tornado developed just prior to 1820 UTC, after two WRSs moved through the convection

3. Synoptic and Mesoscale Analysis

The 1600 UTC Lincoln, Illinois (KILX) sounding confirmed that the instability and shear parameters matched closely to what Murphy et al. (2014), Barker (2006) and Chadwick (1998) had discovered as typical environments for WRS days. Murphy and Knupp (2013) and Barker (2006) found that the environments that appeared to be most conducive for WRS interaction were highly dynamic, and contained low convective available potential energy (CAPE) and relatively high shear. Some corresponding calculations from the 16 UTC KILX sounding were:

- Mixed-layer CAPE - 1313 Jkg-1
- 0-1km shear - 19 ms-1 (37 kts),
- 0-6km shear - 37 ms-1 (71 kts)
- 0-1km storm-relative helicity - 318 m2s-2

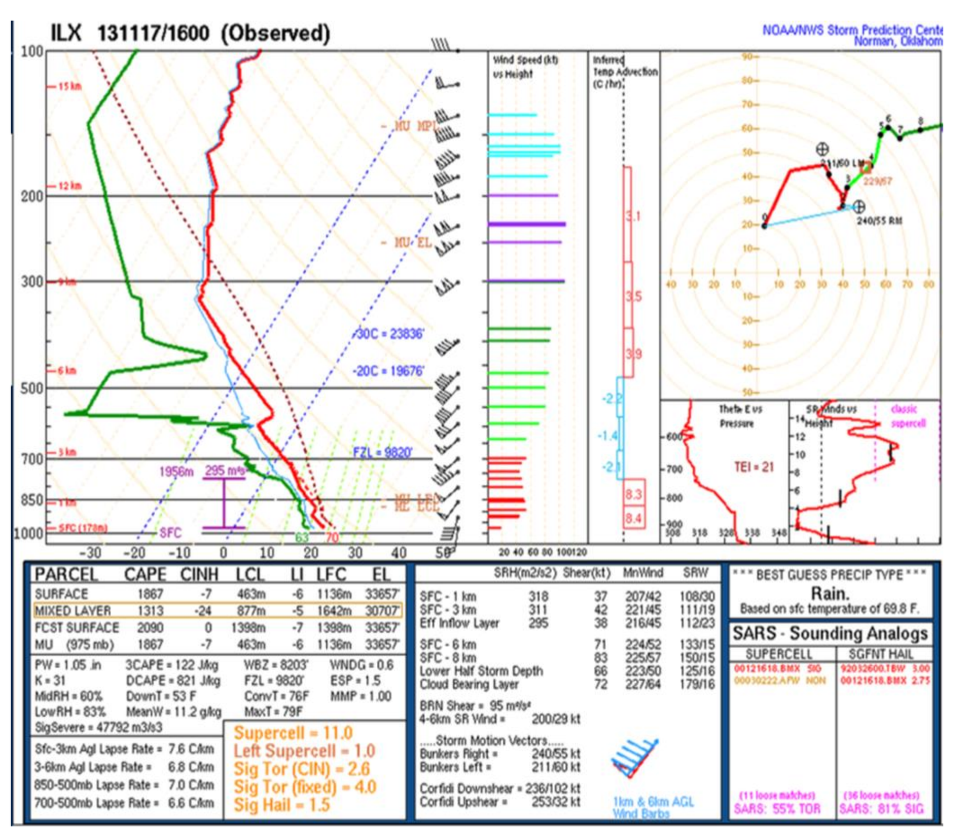

KILX 1600 UTC Sounding, 17 Nov 2013.

Chadwick (1998) found that wave segments often appeared to be linked to a jet streak evident in GOES 6.7 µm imagery (left figure). KILX WSR-88D VAD wind profiler data (right figure) from the time of the tornado also confirmed the presence of a 56 ms-1 (109 kt) jet passing above the tornadic supercell during the time it struck Washington, Illinois.

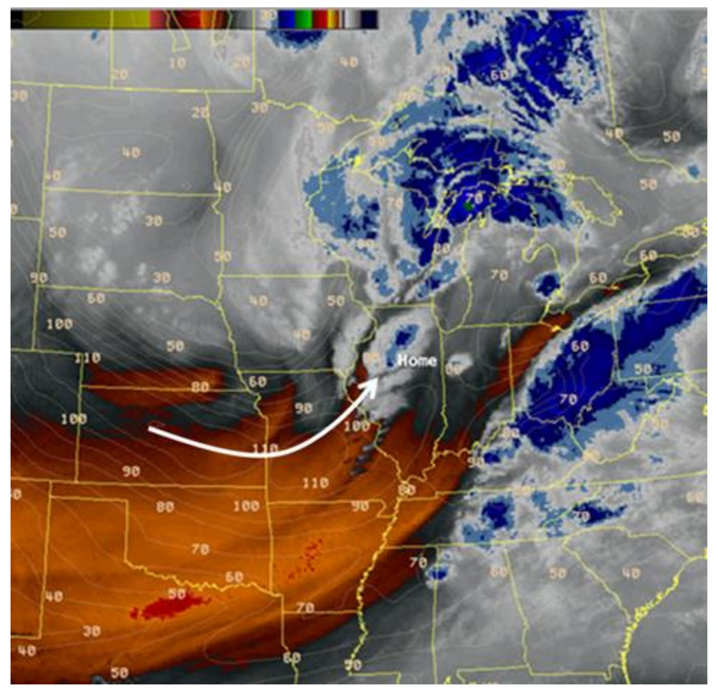

GOES 6.7 µm image and RUC 400-hPa 0-hr wind speed (dotted tan – 10-kt contour interval) 1600 UTC 17 Nov 2013. "Home" marks Washington, Illinois

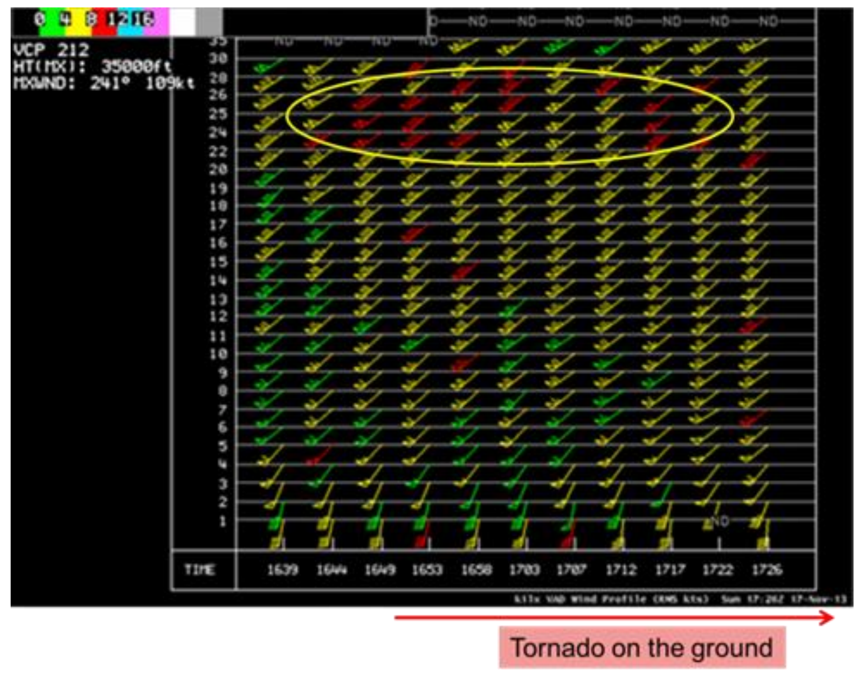

KILX VAD wind profile – 1639 UTC to 1726 UTC.

4. Radar Analysis

During post-event analysis, there appeared to be evidence of two WRSs interacting with the parent supercell to possibly alter the near-storm environment in favor or tornadogenesis and/or mesocyclone intensification. It is hypothesized that the first WRS (WRS 1) played a role in triggering tornadogenesis between 1630 and 1649 UTC, while the second WRS (WRS 2) may have triggered an abrupt intensification of the tornado just prior to it producing EF-4 damage across Washington, Illinois, after 1700 UTC. That was the only period of EF-4 damage that the tornado produced during its life cycle.

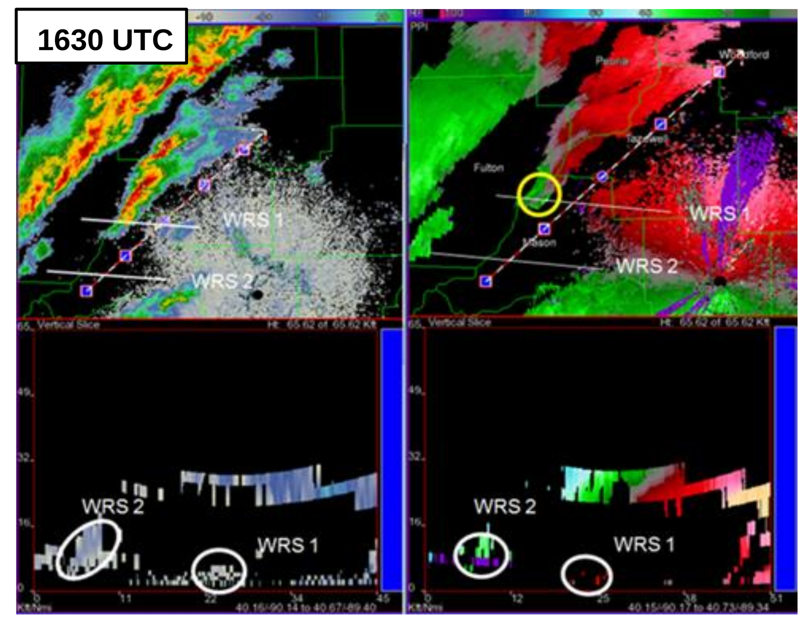

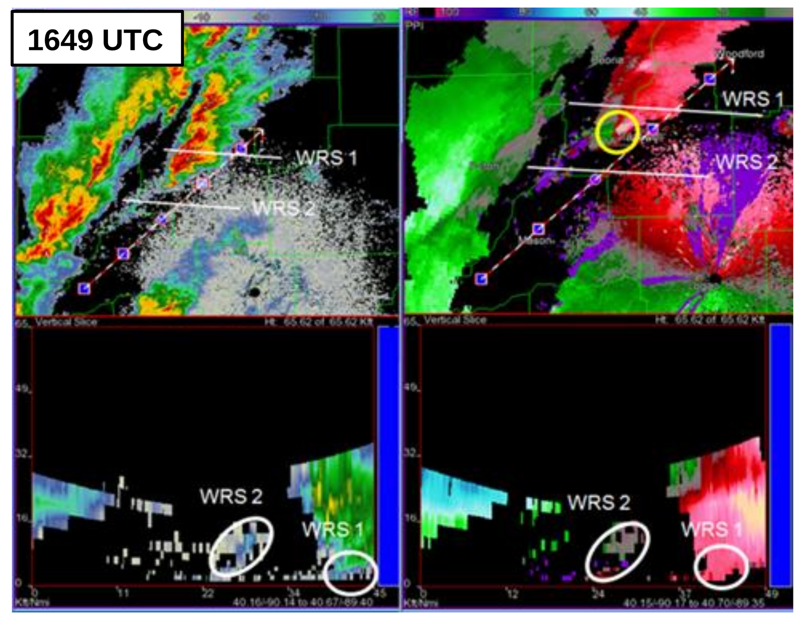

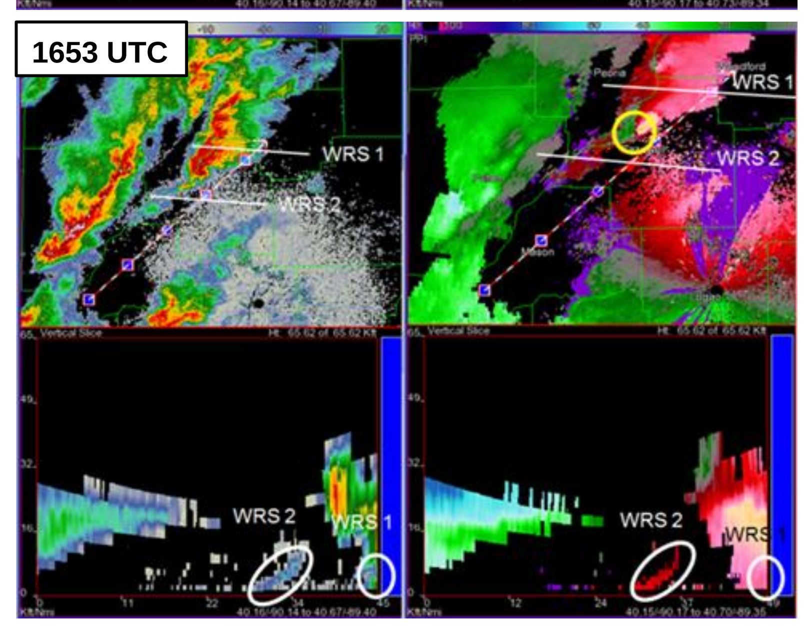

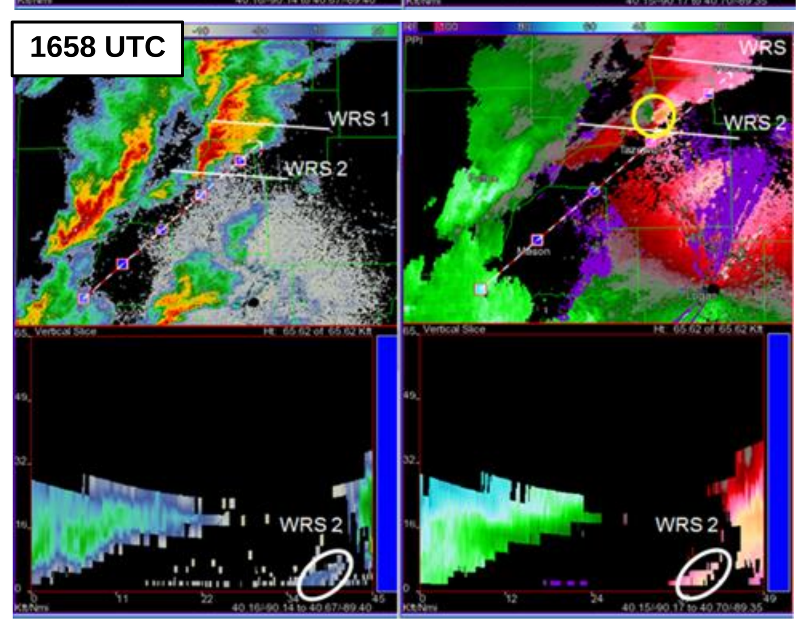

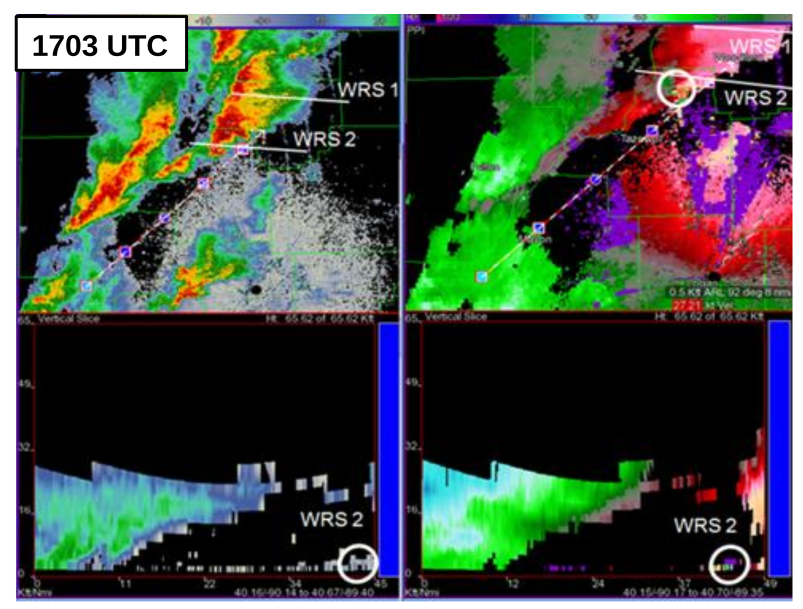

- *FSI images of KILX Z (left half) and V (right half)*
- *Time labeled in upper left corner of each image on 17 Nov 2013.*
- *Top portions of each image are 0.5° Z and V, while the bottom portions of each image are vertical cross sections along the SW-NE-oriented cross-section line displayed in top images.*
- *White circles in the bottom portions of each image show the location of the WRSs (WRS 1 and WRS 2) in cross section.*
- *The yellow circle in the upper right of each image highlights the mesocyclone in the supercell.*

Notable characteristics of these WRSs:

1. A depth of 2-3km.
2. A descending trajectory toward the ground as they neared interaction with the supercell.
   - Possibly due to rear-flank downdraft influence

5. Rotational Velocity Analysis

Descending intensification of the mesocyclone began immediately after interaction with WRS 1 at 1639 UTC, with tornadogenesis delayed by around 10 minutes. The tornado produced mainly EF-0 and EF-1 damage until the intersection of WRS 2 with the tornadic mesocyclone around 1658 UTC. The figure below shows the immediate quantitative intensification of the rotational velocities below 5 km, with more dramatic intensification below 3 km. The last 3 images in the radar analysis section of this poster show the qualitative increase in rotation in the KILX V at 0.5° (images labeled 1653 UTC, 1658 UTC and 1703 UTC).

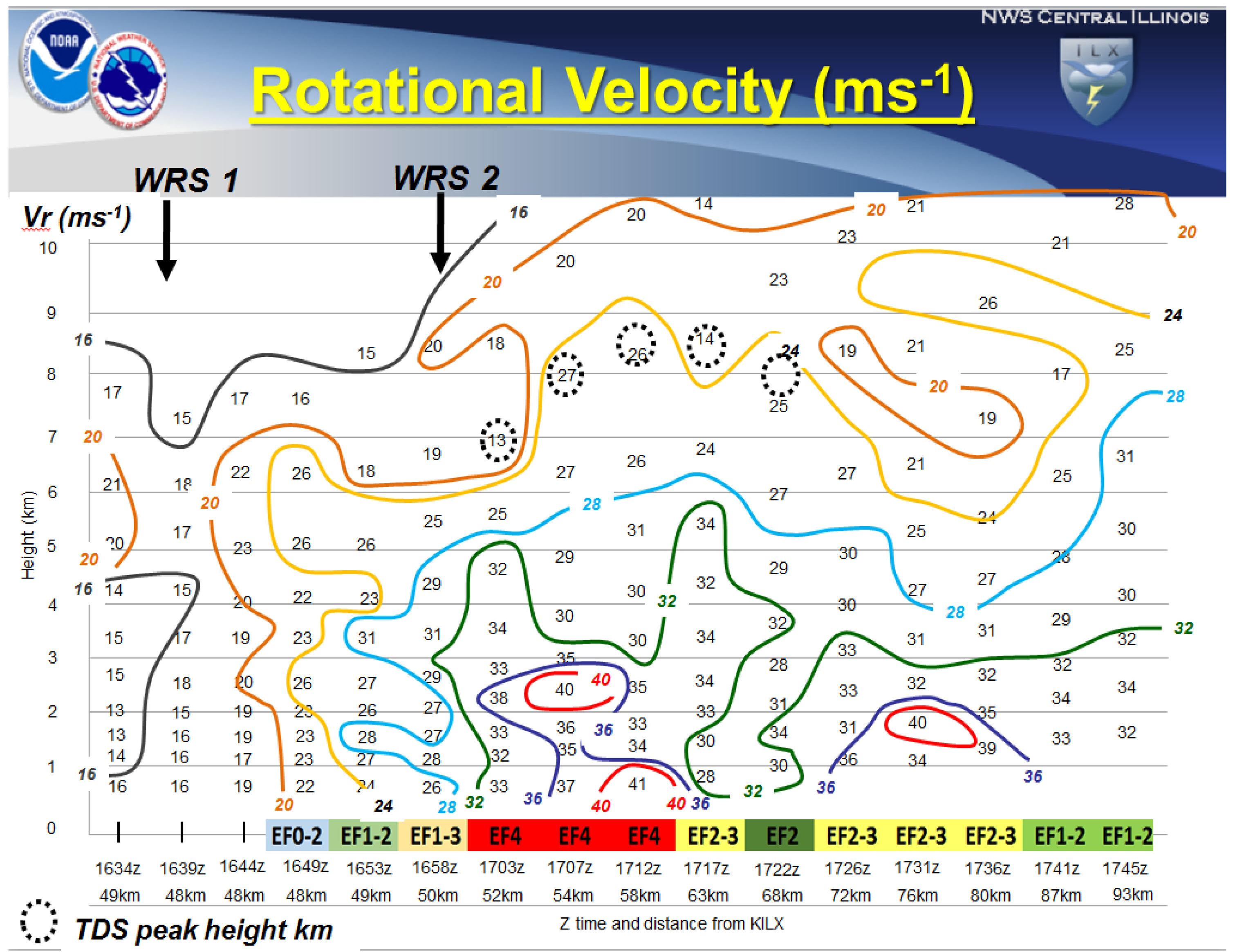

Rotational velocity diagram (ms-1). Colored lines show rotational velocity in increments of 4 ms-1. Increasing height (km) on left side. Across bottom: Increasing time by volume scan, EF rating of tornado, and distance from the KILX radar. Time of interaction with WRS 1 and WRS 2 indicated by the black arrows at the top of the diagram.

There is also direct video evidence of the evolution of the tornado funnel during the period of time surrounding the intersection of WRS 2 and the tornadic supercell, as documented in the two figures below. The figures are video clip snapshots that specifically show the dramatic visual intensification of the tornado circulation as it went from a barely visible condensation funnel around 1659 UTC to a 500-meter (0.3 mile) wide tornado producing EF-4 damage by 1704 UTC.

Snapshot from Clint Plunk video of the tornado near Farmdale Park to the SW of Washington, Illinois at 1659 UTC, just prior to interaction with WRS 2.

Snapshot from anonymous video of the tornado near SW side of Washington, Illinois at 1704 UTC, after interaction with WRS 2.

6. Future Work

(1) Apply radar analysis WRS detection techniques in real time to increase tornado warning lead time.

(2) Local modeling of this event and other WRS tornado days.

- Attempt to reproduce and determine the origin of the WRS elements or gravity waves.

7. References

Barker, L.J., 2006: A Potentially Valuable WSR-88D Severe Storm Pre-cursor Signature in Highly Dynamic, Low Cape, High Shear Environments. Preprints, 23rd Conf. on Severe Local Storms, St. Louis, MO, Amer. Meteor. Soc.

Chadwick, R.B., 1998: The Wind Profiler Demonstration Network. Extended Abstracts, Symp. on Lower Tropospheric Profiling: Needs and Technologies, Boulder, CO, Amer. Meteor. Soc.

Coleman, T.A., and K.R. Knupp, 2006: The Interaction of Gravity Waves with Tornadoes and Mesocyclones: Theories and Observations. Preprints, 23rd Conf. on Severe Local Storms, St. Louis, MO, Amer. Meteor. Soc.

Coleman, T.A., and K.R. Knupp, 2008: The Interactions of Gravity Waves with Mesocyclones: Preliminary Observations and Theory. Mon. Wea. Rev., 136, 4206–4219.

Murphy, T.A., K.R. Knupp, 2013: Prevalence and Characteristics of Atmospheric Waves in Severe Weather Environments. Preprints, 94th Annual Conf., Atlanta, GA, Amer. Meteor. Soc.

Murphy, T.A., R.A. Wade, T.A. Coleman, and K.R. Knupp, 2014: Observations and analysis of reflectivity segments interacting with a quasilinear convective system. Currently in review at Mon. Wea. Rev.